

Received May 31, 2020, accepted June 23, 2020, date of publication July 6, 2020, date of current version July 21, 2020.

Digital Object Identifier 10.1109/ACCESS.2020.3007148

# Extended Worst-Case OSNR Searching Algorithm for Optical Network-on-Chip Using a Semi-Greedy Heuristic With Adaptive Scan Range

YONG WOOK KIM<sup>1</sup>, (Student Member, IEEE), JAE HOON LEE<sup>2</sup>, (Member, IEEE),  
AND TAE HEE HAN<sup>3</sup>, (Member, IEEE)

<sup>1</sup>Department of Electrical and Computer Engineering, Sungkyunkwan University, Suwon 16419, South Korea

<sup>2</sup>Memory Division, Samsung Electronics, Hwaseong 18448, South Korea

<sup>3</sup>Department of Semiconductor Systems Engineering, Sungkyunkwan University, Suwon 16419, South Korea

Corresponding author: Tae Hee Han (than@skku.edu)


This work was supported in part by the National Research Foundation of Korea(NRF) grant funded by the Korea government (MIST) under Grant 2020M3H2A1076786, and in part by the MOTIE(Ministry of Trade, Industry and Energy) and KSRC (Korea Semiconductor Research Consortium) support program under Grant 20010560.

**ABSTRACT** The advances in silicon photonics technology have facilitated the realization of optical network-on-chips (ONoCs) to cope with the physical limitations of metal interconnections in traditional CMOS integrated circuits. As the performance and reliability of optical links are adversely affected by insertion losses and crosstalk, which inevitably occur during the propagation of optical signals, optimizing the power of a laser source requires a sophisticated analysis of the optical signal-to-noise ratio (OSNR). Calculating the worst-case OSNR for all possible communication links in an ONoC is an NP-hard problem even under the assumption of a single-wavelength laser source. Moreover, when expanding the design space by accommodating wavelength-division multiplexing (WDM), semiconductor optical amplifier (SOA), diverse topologies, and the associated router architectures, the computational complexity becomes excessive. Therefore, in this study, we propose an extended worst-case OSNR search algorithm (EWOSA) that significantly reduces the computational burden through a preprocessing algorithm that reduces the number of candidate paths when the combined effect of the insertion loss and crosstalk on the OSNR is considered. Simulation results demonstrate that the EWOSA can identify approximately 0.18 dB lower worst-case OSNR than the existing formal worst-case analysis method in  $8 \times 8$  mesh-based ONoC, and this improvement in OSNR accuracy becomes more apparent (up to 4.81 dB) when SOAs are deployed in ONoCs. Furthermore, the EWOSA can be used for OSNR optimization, owing to its rapid analysis speed and generality.

**INDEX TERMS** Optical network-on-chip, OSNR, secondary effect of crosstalk noise, semi-greedy heuristic, worst-case searching.

## I. INTRODUCTION

A network-on-chip (NoC) is a scalable on-chip communication infrastructure that was proposed to resolve communication bottlenecks due to the ever-increasing number of processor cores and massive data traffic caused by intensive data accesses and parallelism. Although the conventional NoC based on metal interconnections offers scalable on-chip communication, it suffers from significant challenges in terms of performance and power consumption, owing to its limitation

The associate editor coordinating the review of this manuscript and approving it for publication was Leo Spiekman .

in the scaling of the feature size. Fortunately, with the recent advances in nanoscale silicon photonics technology, a photonic-link-based optical network-on-chip (ONoC) has emerged as an alternative to achieve higher communication performance and energy efficiency than those of electrical links [1], [2].

The crossing of signals owing to the planar structure of the optical elements in an ONoC, the imperfection of optical elements and the scattering of the light signal cause attenuation and noise in the intensity of the optical signal. Insertion loss and crosstalk noise are two dominant factors that adversely affect reliable detection at the

optical receiver. Therefore, determining the worst-case optical signal-to-noise ratio (OSNR), considering the accumulated effect of insertion loss and crosstalk noise in the entire network, is a crucial step when constructing an ONoC [3].

A brute-force approach of comparing all possible communication paths in an ONoC to determine the worst-case OSNR is an NP-hard problem. Moreover, owing to the resonant structure of microring resonators (MRs), numerous iterative computations are required until the optical signal is stabilized in the optical router. Hence, the number of computations increases significantly as the network size increases. The signal power of the OSNR is determined regardless of other communications when the source and destination of the designated optical link are determined, and the noise power is determined by all the signal paths that cause crosstalk in the designated optical link. Therefore, the calculation of noise power significantly affects the computational complexity. The signal paths that cause the maximum noise power can be inferred from the common characteristics of ONoCs with different topologies experiencing insertion loss and crosstalk. Furthermore, the worst-case OSNR determines the minimum required output power of the laser light source. As the sensitivity improvement of the photodetector is limited, and the laser source accounts for a considerable proportion of the total power consumption of the ONoC, analyzing the worst-case OSNR has a significant effect on estimating the total power consumption, heat dissipation, and implementation cost of the ONoC [1], [4], [5]. In particular, as the laser power consumption accounts for a significant proportion of the total power consumption of the entire optical network [6], an accurate worst-case OSNR analysis is required for precise power allocation.

Previous studies demonstrated that the OSNR of a folded-torus-based ONoC is lower than 0 dB at a network size of  $12 \times 12$  or larger; therefore, the intensity of noise power is higher than that of the signal power, and the reliable detection of the signal is impossible. Various OSNR optimization techniques incorporating wavelength-division multiplexing (WDM) or semiconductor optical amplifier (SOA) have been studied to compensate for the above limitation. However, the analysis of the worst-case OSNR of networks using these optimization techniques has not been considered in depth. Moreover, previous studies on the analysis of the worst-case OSNR in an ONoC have not addressed the diverse aspects of optical networks, such as topologies.

In this context, we propose an extended worst-case OSNR searching algorithm (EWOSA) to achieve enhanced accuracy and availability. The proposed EWOSA adaptively adjusts the range of candidate groups that might cause the worst-case OSNR of an ONoC by utilizing the common characteristics of the ONoCs with diverse topologies and considering a trade-off between accuracy and computational complexity. Consequently, the EWOSA is compliant with topology-specific OSNR optimization algorithms and can be applied to optical networks incorporated with SOA and WDM. In addition, we describe an OSNR-optimized

low-power ONoC architecture with the EWOSA tailored to the requirements of various applications.

The remainder of this article is organized as follows: The related studies and background are described in Section II. Section III presents the main algorithm proposed in this article, the EWOSA, and describes the techniques for applying it to OSNR-optimized ONoCs. Simulation results and analyses under various conditions are described in Section IV. Finally, the conclusion is presented in Section V.

## II. RELATED WORK

All the signals passing through optical networks experience insertion losses, which attenuate the signal intensity depending on the physical properties of the optical devices in the signal path. Additionally, at the intersection of the waveguide and MR switch, at which the optical signal crosses the other signal paths, the signal leaks into undesired paths owing to the scattering of light and the mismatch of the resonance frequency between the signals in the MR switch, which acts as crosstalk noise.

The analysis of OSNR in ONoCs should focus on insertion loss and crosstalk, which have the greatest effect on signal and noise power, respectively. Accordingly, recent studies have focused on both the analysis method and reduction technique of insertion loss and crosstalk.

In [7] and [8], low-power non-blocking optical routers were proposed to minimize insertion loss. The proposed Cygnus and optical turnaround routers (OTARs) reduced the total power consumption of the entire optical network layer by using a smaller number of MRs with an insertion loss lower than that of the conventional crossbar router. Nikdast *et al.* presented a crosstalk analysis method in which optical signals of various wavelengths interfere with each other in mesh, folded-torus, and fat-tree topologies for large-scale WDM-based ONoCs [9]. They compared the worst-case OSNRs in different topologies and analyzed the change in OSNR with a varying number of wavelengths in a WDM environment.

As the calculation of insertion loss and crosstalk of thousands of optical elements requires a significantly high computational complexity, recent studies have focused on simplifying the worst-case OSNR computations, which is critical in determining the minimum power required for the laser source.

An analytical method to calculate the crosstalk and insertion loss considering the individual optical elements and network structure was proposed in [10]. This method demonstrated how to determine the OSNR depending on the network sizes and the structure of the optical router. The worst-case OSNR link, affected by the number of crosstalk sources and insertion loss, existed among the first to third-longest paths in mesh-based ONoCs. In [11], Xie *et al.* presented analytic expressions for the change in signal intensity and noise power caused by insertion loss and crosstalk when a signal passes through optical elements depending on the switching state of the allocated router. They formally derived an OSNR

equation for an ONoC with mesh topology and analyzed the worst-case OSNR under various network sizes and signal power losses.

In [12], Nikdast *et al.* analyzed the worst-case OSNR of an ONoC with a folded-torus topology using the same mathematical model as in [10] and presented the crosstalk and loss analyses platform (CLAP), which analyzes crosstalk noise and insertion loss. Using the proposed model, they indicated that the worst-case OSNR in the folded-torus-based ONoC could occur on one of the longest paths ranked from first to fourth. Additionally, they concluded that crosstalk noise significantly limits the scalability of ONoCs in terms of network size. In [9], CLAP was extended to include fat-tree-based and WDM-based ONoCs with an OTAR; however, crosstalk noise was still considered an obstacle for the scalability of ONoCs.

In [10] and [12], the authors considered that the worst-case OSNR occurs when the sources of crosstalk noises are located close to the optical signals. They considered that the power of the crosstalk from routers more than two hops away from the desired signal path is less than that of the crosstalk from a router adjacent to the signal path because the insertion loss coefficient is multiplied more than once. The advantage of this approach is that by simplifying the OSNR calculation via eliminating unnecessary signals, the increase in network size has only a slight effect on the computational complexity. In particular, the OSNR equation is derived from the coefficients of optical elements and the network size considering the insertion loss and crosstalk noise of the longest path. However, this method can only be applied to certain topologies, such as mesh or folded torus.

The intensity of the crosstalk tends to be attenuated by the insertion loss according to the distance from the desired optical link to the optical router at which the crosstalk is introduced. However, as the minimum attenuation of the crosstalk due to insertion loss is only 3.3 % per router, crosstalk from routers more than two hops away from the optical link cannot always be ignored.

Furthermore, the crosstalk noise from the nodes more than two hops away from the desired optical link can accumulate with other noises having a similar phase response, resulting in a noise power higher than the optical signal power. The experimental results in [13] demonstrated that the worst-case OSNR can be lower than 0 dB, indicating that the noise power is higher than the signal power for network sizes larger than  $12 \times 12$  in the mesh-based ONoC. Considering these results between the signal paths that cause crosstalk noise, we conclude that we cannot ignore the scenario in which the crosstalk noise coefficient is multiplied more than once. Thus, the accumulated noise power involving diverse interactions among different crosstalks in large-scale ONoC should be considered. Additionally, the signal paths in which the crosstalk noise coefficient is multiplied more than once have greater effects as the number of signal crossings increases with larger network size and heavier traffic.

The OSNR-related works discussed here were limited to ONoCs based on specific topologies. Furthermore, analyzing

the OSNR in detail was difficult because signal paths in which the crosstalk noise coefficient is multiplied more than once were ignored for the convenience of calculation. In this article, we propose a general-purpose and scalable OSNR analysis algorithm that can be applied to various topologies and network sizes while considering secondary crosstalk noise, which has not been addressed in previous studies.

### III. EWOSA

The EWOSA adopts a semi-greedy approach to prevent an excessive increase in computational complexity and missing the global optimum. Unlike general greedy algorithms, the semi-greedy heuristic in our EWOSA significantly decreases the computational complexity by specifying the worst-case candidate group consisting of strictly selected signal paths, considering the characteristics of the optical signal and the effects of insertion loss and crosstalk. The worst-case path selected among the worst-case candidates minimizes the probability of falling into the local minimum through multiple subsets using various searching conditions. Moreover, router-level calculation using the linearity of optical elements significantly decreases the computational complexity. The EWOSA dramatically reduces the computational complexity while preventing the degradation in the accuracy of the OSNR because of the semi-greedy approach through appropriate searching conditions, enabling a rapid and accurate simulation at the design stage of the ONoC architecture. Section III.A discusses the input-to-output ratio table of a single router prepared before EWOSA execution as well as the calculation of the OSNR during the EWOSA execution. Section III.B describes the overall operation of the algorithm in three steps.

#### A. OSNR CALCULATION METHOD

Here, we describe a method to dramatically decrease the number of repetitive operations by abstracting the operation of the optical element level to the router level. The optical elements required to calculate the OSNR are determined by the switching state of the optical routers along the signal path. Therefore, if the input-to-output ratio of the signal intensity at each port according to the switching state of the router is calculated in advance and stored in a lookup table (LUT), the output power according to the input power of the signal path can be easily calculated by referring to the corresponding ratio in the table.

A certain optical signal in a specified path acts as crosstalk in all the other paths. Its noise power is considered in all the optical elements where crosstalk can occur; hence, even the designated signal path can be affected by the secondary effect of the crosstalk caused by itself. Therefore, the input-to-output ratio of the noise power in the router is calculated by considering the crosstalk of all the optical elements according to the MR states independent of the signal route. In contrast, the signal power at the destination is calculated by considering the total insertion loss through all the optical elements present in the routing path. Thus, the ratio of the loss and

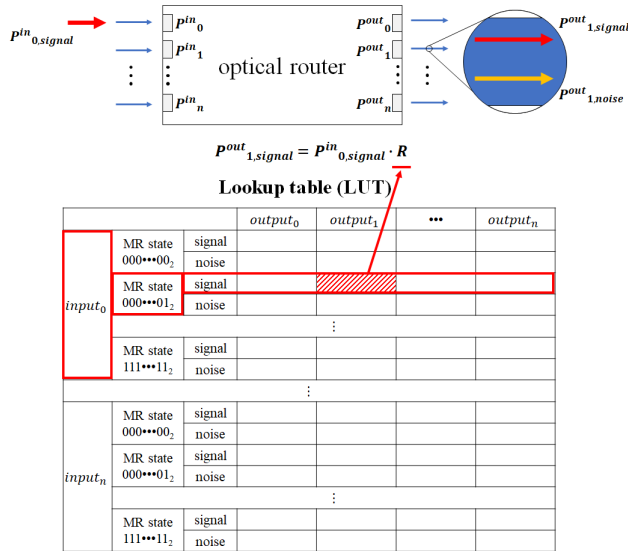


**FIGURE 1.** Example of the power calculation of the optical signal using the LUT.

crosstalk between each input and output port of the router is tabulated according to the assigned switching state.

Let the signal and noise powers of the  $i$ th input port be  $P_{i,signal}^{in}$  and  $P_{i,noise}^{in}$ , respectively, and the signal and noise powers of the  $j$ th output port be  $P_{j,signal}^{out}$  and  $P_{j,noise}^{out}$ , respectively. Fig. 1 shows an example of calculating  $P_{1,signal}^{out}$  when  $P_{0,signal}^{in}$  is attenuated while passing through a single router if the input-to-output power coefficient is assumed to be  $R$  when the corresponding MR state is  $000 \dots 1_2$ .

In an ONoC using a single-mode wave, the optical elements including MR switches have linear properties [14]. Thus, the total loss from the corresponding input to the desired output ports of the router can be obtained by considering the number of elements and waveguide length according to the allocation of MR switches. Moreover, the superposition principle enables the input-to-output ratio in the router, which is the signal attenuation ratio between its input and output ports, to be calculated independently.

Fig. 2(a) depicts the optical elements through which the optical signal passes from the west to east ports of a Crux router in a mesh-based ONoC. The signal path passes through the four through-state MRs. When the radius of the MR switch is  $5 \mu\text{m}$ , as used in [15], the waveguide of the optical link should be longer than  $46.5 \mu\text{m}$ . By considering these values and assuming that the insertion loss coefficients, i.e., the MR loss coefficient of the OFF state parallel element  $L_{OFF,pe}^{MR}$ , the MR loss coefficient of the crossing element  $L_{OFF,ce}^{MR}$ , and the loss coefficient of the waveguide  $L^{WB}$  are  $-0.005$ ,  $-0.04 \text{ dB}$ , and  $-0.274 \text{ dB/cm}$ , respectively, the total insertion loss of the corresponding signal path can be calculated as approximately  $-0.14 \text{ dB}$  using (1).

$$Total\ loss = (1 - L_{OFF,pe}^{MR}) \cdot (1 - L_{OFF,ce}^{MR})^3 \cdot (1 - 46.5 \times 10^{-4} \cdot L^{WB}) \quad (1)$$

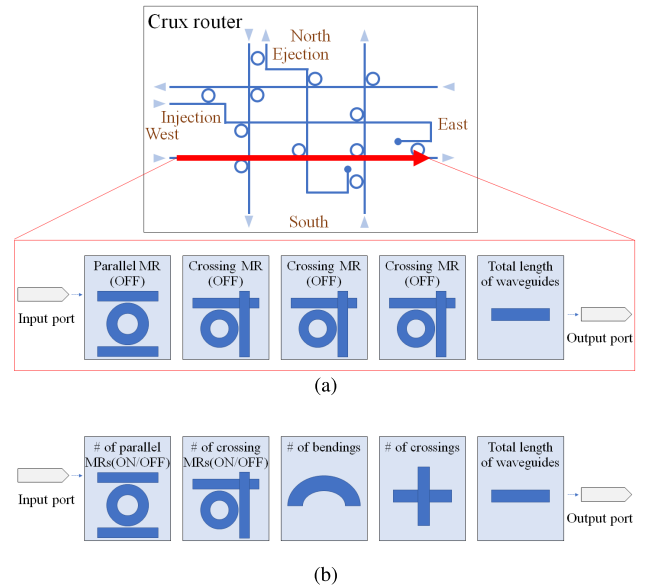


**FIGURE 2.** Optical elements in Crux router through which (a) the specific optical signal passes, (b) general optical signal passes.

Thus, all the elements considered in calculating the insertion loss of the signal path can be represented by the number of independent optical elements (Fig. 2(b)). Since each optical signal can be linearly calculated, independently of the order of the optical elements through which it passes, the intensity of the optical signal is calculated using the number and length of the optical elements through which it passes.

Finally, we can obtain the OSNR of the optical link through the signal and noise powers according to the signal propagation in each router calculated by referring to the LUT. Because predicting the phase of all the optical signals in the ONoC is difficult, and the objective of the EWOSA is to search for the worst-case scenario, we ignored the phase difference of the different crosstalks. Hence, the cumulative computation of each crosstalk is performed by the addition operation due to the compensation interference. If the signal and noise powers originating from the  $i^{th}$  input port of the  $n$ -port optical router are  $P_{signal,i}^{in}$  and  $P_{noise,i}^{in}$ , respectively, and the signal and noise powers arriving at the  $j^{th}$  output port are  $P_{signal,j}^{out}$  and  $P_{noise,j}^{out}$ , respectively, and denoting the MR state of the corresponding router as  $ms$  and the input-to-output ratios of the signal and noise powers from the input port  $i$  to the output port  $j$  as  $R[i][ms][signal][j]$  and  $R[i][ms][noise][j]$  in the LUT, respectively, we obtain the following equations:

$$P_{signal,j}^{out} = P_{i,signal}^{in} \cdot R[i][ms][signal][j], \quad \text{for } \forall i, j \in \{1, 2, 3, \dots, n\} \quad (2)$$

$$P_{noise,j}^{out} = \sum_{k=0}^n (P_{k,signal}^{in} + P_{k,noise}^{in}) \cdot R[k][ms][noise][j] \quad \text{for } \forall i, j \in \{1, 2, 3, \dots, n\}. \quad (3)$$

An SOA can be deployed to compensate for the attenuation of the signal intensity due to insertion loss. Thakkar increased



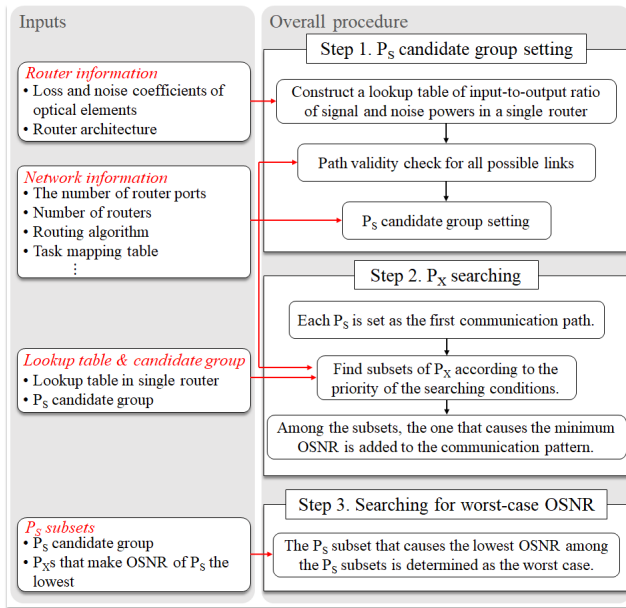


FIGURE 3. Process of the EWOSA.

the laser power savings in an ONoC by 31.5 % with a low latency overhead using an SOA [5]. In [16], the authors proposed a hybrid ONoC architecture using an SOA to decrease the total power consumption and mitigate the OSNR degradation, considering the network size scalability without increasing the output power of the laser source. The above two studies concluded that an SOA could decrease the OSNR while also reducing the overall power consumption of the optical network. Thus, after calculating the internal optical signal power of the router using the LUT, the signal compensation due to the SOA placed in each router port is additionally calculated considering the SOA gain. We considered that an SOA with a gain of 1 is placed in a port with no SOA. Since the propagated signal renews the signal intensity of the input ports of adjacent routers, this operation is repeated until the effect of each router on the others is stable. The computational complexity of these operations is very low compared with that caused by the iterative operation at the optical element level.

### B. ALGORITHM DESCRIPTION

The EWOSA is performed in three steps (Fig. 3). First, we introduce the following two notations:

$P_S$ : the designated optical signal path under the OSNR analysis, and

$P_X$ : the crosstalk path to the  $P_S$ .

The EWOSA determines a  $P_S$  candidate group that can cause the worst-case OSNR and  $P_X$ s that minimize the OSNR at the destination node of each  $P_S$  in the candidate group. This process is divided into steps 1 and 2. In particular, in step 2, involving determining the  $P_X$ s, which is the probability of the local minimum is minimized by using a semi-greedy heuristic that determines a candidate group with a specific search range and obtains optimum subsets using various searching conditions of the candidate groups. This method enables the derivation of a very accurate worst-case OSNR

while maintaining a low computational complexity, which is an advantage of the greedy algorithm.

The first step is to prepare the input-to-output ratio table of a single router. Subsequently, the  $P_S$  candidate group is set according to the  $P_S$  searching condition, and the OSNR is calculated by referring to the corresponding table. The second step is to select the  $P_X$ s that minimize the OSNR of each  $P_S$  among the  $P_S$  candidate groups according to the  $P_X$  searching condition and calculate the corresponding OSNR. In the third step, the  $P_S$  and corresponding  $P_X$ s that cause the lowest OSNR among the calculated OSNRs are determined as the worst case, and the OSNR is considered as the worst-case OSNR.

#### 1) $P_S$ CANDIDATE GROUP SETTING

According to the  $P_S$  searching condition, the EWOSA exhaustively selects source and destination pairs from all the communicable nodes until no more selectable nodes are available. Subsequently, the algorithm adds selected nodes consisting of source and destination pairs to the  $P_S$  candidate group. If task mapping has been performed beforehand, only the source and destination pairs in the task mapping table are added to the candidate group. We propose a pathfinding algorithm, which is a sub-algorithm of the EWOSA, to track the signal path determined by the source and destination node pair and the changed MR state and port occupancy state. Note that the optical signal path to be analyzed does not violate circuit switching in advance. For this prerequisite operation, the pathfinding algorithm involves receiving source and destination nodes as arguments and verifying the path validity.

The process of the pathfinding algorithm is described in Algorithm 1. The port of each router has a one-bit flag used to check if the corresponding port is occupied. The flag is initialized to zero. Whenever each signal path passes through the router, the flag of the router port through which the signal passes is changed from zero to one. When communication ends or the corresponding signal path is excluded from the communication pattern, the flags corresponding to the signal path change to zero. The pathfinding algorithm tracks the routers one at a time according to the routing algorithm from the input source node to the destination node to check the path validity. It determines that the signal path is invalid if the signal must pass through a port with a flag of one, or the signal path is impossible to match with the destination node according to the routing algorithm. The pathfinding algorithm marks the connection information of the input and output ports of each router so that the ports of the router through which the corresponding signal path passes can be easily located. The MR state is simply changed through the information marked on each router.

#### 2) $P_X$ SEARCHING

$P_X$  searching is the process of determining the signal paths that cause the minimum OSNR for each  $P_S$  candidate obtained in step 1. The pathfinding algorithm is performed in

**Algorithm 1** Pathfinding Algorithm

---

**Input** integer source\_node, integer destination\_node  
**Output** boolean validity

- 1: current\_router = the router connected to source\_node
- 2: current\_port\_in = the input port of the current\_router originating from the source\_node
- 3: current\_port\_out = the output port of the current\_router determined by the routing algorithm
- 4: **while** the current\_port\_out does not indicate the destination\_node **do**
- 5:   **if** any flag of current\_port\_in and current\_port\_out is one or current\_port\_out is -1 **do**
- 6:     change all the flags to zero
- 7:     remove the input and output marks that changed from this algorithm call
- 8:     validity = 0 // 0 indicates that the path is invalid
- 9:   **else**
- 10:    change the flags of the input\_port and output\_port to one
- 11:    mark that the input and output ports are connected
- 12:    prior\_router = current\_router
- 13:    current\_router = the router connected to the output\_port of the current\_router
- 14:    current\_port\_in = the input port of the current\_router originating from the prior\_router
- 15:    current\_port\_out = the output port of the current\_router determined by the routing algorithm
- 16:    **end if**
- 17:    **end while**
- 18:    validity = 1 // 1 indicates that the path is valid

---

the same manner as in step 1. In addition, if task mapping has been performed beforehand, only the source and destination pairs that can be communicated in the task mapping table are limited to the search range as  $P_X$ .

The EWOSA is based on a semi-greedy algorithm that determines the signal path causing the worst-case OSNR among the candidate groups searched in advance through the searching conditions. When a signal path is connected to the processor nodes, the circuit switching and structural characteristic of the planar optical elements in the ONoC prevent multiple signal paths that must pass through the same path. Therefore, setting the  $P_X$  searching condition to determine the  $P_X$  with a high probability of being the worst case is essential. The  $P_X$  searching condition can be divided into searching and searching-stop conditions. The two conditions define the search range of each  $P_X$ . The search condition is determined by the common characteristics of the signal paths that cause the worst-case OSNR in the optical network to determine a signal likely to be the worst case. The searching-stop condition reduces the total simulation time by limiting the number of  $P_X$  candidate groups.

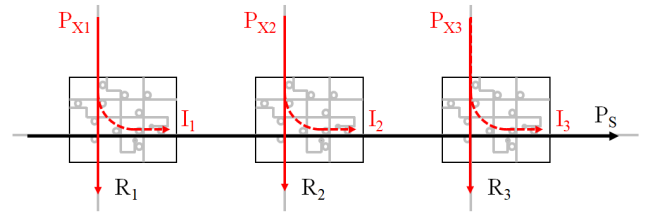


**FIGURE 4.** Example where multiple  $P_X$ s causing crosstalks on a single  $P_S$  in a mesh-based ONoC employing Crux routers.

The searching-stop condition is determined using the intensity of the crosstalk caused by the  $P_X$  candidate group determined so far, considering the maximum values of insertion loss and crosstalk noise that can occur in a router.

The OSNR of the destination node of a  $P_S$  is determined by the power of the optical signal passing through the  $P_S$  and the power of the crosstalk noise accumulated in the  $P_S$ . The signal power attenuated due to the insertion loss of the  $P_S$  is determined by the optical elements passing through the  $P_S$ . Consequently, only the intensity of the crosstalk noise that can be exerted on the  $P_S$  affects the OSNR in the  $P_X$  searching step.

The crosstalk noise introduced at the router at which  $P_S$  and  $P_X$  intersect experiences insertion loss in the mesh-based ONoC (Fig. 4). Assuming that the insertion loss coefficients of all the Crux routers are the same as  $L$  ( $0 < L < 1$ ). Let the crosstalk intensities of  $P_{X1}$ ,  $P_{X2}$ , and  $P_{X3}$  are  $I_1$ ,  $I_2$ , and  $I_3$  at the routers  $R_1$ ,  $R_2$ , and  $R_3$ , respectively. Assuming  $I_1$ ,  $I_2$ , and  $I_3$  are identical, the relationship between them can be expressed as (4).

$$I_1 \cdot L^2 < I_2 \cdot L < I_3 \quad (4)$$

Therefore, the fewer routers through which the optical signal passes from the router at which  $P_S$  and  $P_X$  intersect to the destination node of the  $P_S$ , the lower the insertion loss that affects  $P_X$ . This tendency is a common property regardless of the type of optical network. As  $P_X$  begins from the router adjacent to the  $P_S$ , resulting in smaller hop counts and insertion loss, the  $P_X$  is less affected by the insertion loss when the distance between the source of  $P_X$  and the router is decreased. Additionally, because the MRon causes a much larger insertion loss than MRoff, the  $P_X$  that passes through fewer MRons in the drop state experiences a lower insertion loss. However, owing to the circuit switching and structural characteristic of the planar optical elements in the ONoC, communication that requires a long path prevents several candidates that can be the worst-case from being selected, resulting in the deterioration in the accuracy of the EWOSA. Therefore, among the  $P_X$ s causing the same intensity of crosstalk noise, selecting the  $P_X$  via the shorter router as the worst case can reduce the number of signal paths constrained by circuit switching.

Considering the above common characteristics of the ONoC, the searching conditions can be summarized as follows:

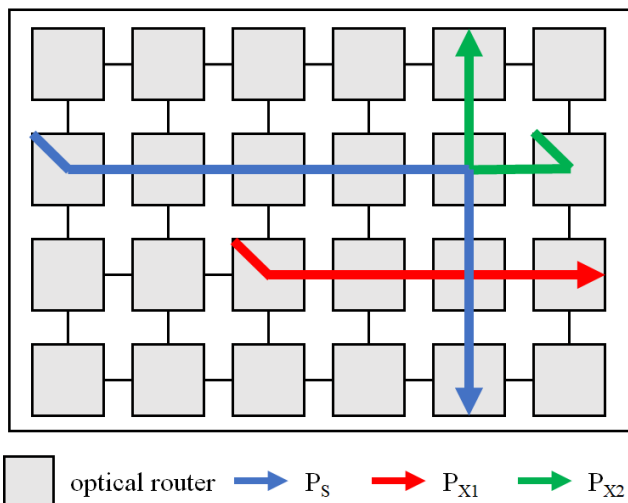


FIGURE 5. Example of two  $P_X$ s introduced in a  $P_S$  in a mesh-based ONoC.

- Search for the  $P_X$  originating from routers with smaller hop counts from the router at which the  $P_S$  and  $P_X$  intersect.
- Search for the  $P_X$  when the location of the crossing router is close to the destination of the  $P_S$ .
- Search for the  $P_X$  that passes through fewer MRs in the drop state until crossing with the  $P_S$ .
- Select the  $P_X$  passing through fewer routers as the worst case among the  $P_X$ s that cause the minimum OSNR.

To reduce the runtime of the EWOSA and search for the reliable worst-case OSNR, the searching-stop condition can be described as follows:

- If the difference between the crosstalk that the  $P_X$  previously selected for the  $P_S$  and the crosstalk that the  $P_X$  currently applies to is lower than the predetermined crosstalk threshold, the EWOSA is terminated.
- The EWOSA is terminated when no more  $P_X$ s are available for the search.

The maximum value of the crosstalk threshold  $T_C$  in the searching-stop condition is an important factor that determines the accuracy and runtime of the algorithm. Hence, it should be considered according to the insertion loss and crosstalk noise coefficient.  $T_C$  is first determined by the magnitude of the effects of the other factors on the size of the crosstalk of the  $P_X$  that is not considered a search condition. A signal with crosstalk as much as the maximum and minimum values of the insertion loss that may occur in a router may exist in the worst-case path whenever the signal path first searched passes through a router. Therefore, when crosstalk is generated in routers crossing with  $P_S$ , there may be a difference as high as the difference between the maximum and minimum values of the crosstalk coefficient that may occur in a router.

Fig. 5 shows an example of  $P_{X1}$  and  $P_{X2}$  that can be selected as candidates causing the worst-case OSNR. In  $P_{X1}$  and  $P_{X2}$ , the distance from each source to the destination of the  $P_S$  is three hops, which satisfies the

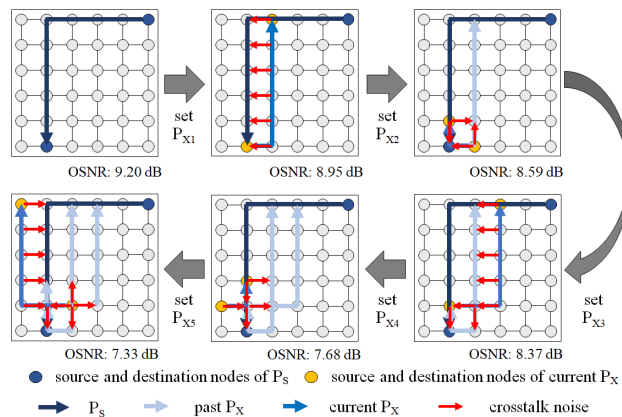


FIGURE 6. OSNR calculation example in the EWOSA for a 6 × 6 mesh-based ONoC.

same searching conditions.  $P_{X1}$  experiences the insertion losses of  $IL_{core \rightarrow east}$ ,  $IL_{west \rightarrow east}$ , and  $IL_{north \rightarrow core}$  until it reaches the destination of  $P_S$ , and  $P_{X2}$  experiences the losses of  $IL_{core \rightarrow west}$ ,  $IL_{north \rightarrow south}$ , and  $IL_{north \rightarrow core}$ . Moreover, when the two  $P_X$ s are crossed, they are affected by different crosstalk coefficients. Therefore, the crosstalk threshold  $T_C(n)$  that changes according to the number of routers,  $n$ , which are counted from the source node of  $P_X$  to the destination node of  $P_S$  is determined by  $C_{th}$  and  $IL_{th}$ , as indicated by (5):

$$T_C(n) = C_{th} + n \cdot IL_{th} \tag{5}$$

where  $C_{th}$  and  $IL_{th}$  are the maximum differences in the crosstalk coefficients and insertion losses that can occur in a single router, respectively.

Fig. 6 shows a subset of  $P_X$  determined by step 2 of the EWOSA in a 6 × 6 mesh-based ONoC. The crosstalk noises that the current  $P_X$  applies to the current optical paths are indicated by red arrows. As the crosstalk noise affects the  $P_S$  and current  $P_X$ s, secondary crosstalk noise is considered with the insertion loss. The magnitude of the OSNR reduced by  $P_{X4}$ , which is two hops from its source to the destination of the  $P_S$ , is greater than the magnitude of the OSNR reduced by  $P_{X1}$ ,  $P_{X2}$ , and  $P_{X3}$ , which are one hop from their source. This indicates that the effect of the insertion loss does not depend only on the number of routers the signal passes through, and this tendency indicates that the  $T_C$  can be determined by considering the maximum and minimum insertion losses and the crosstalk noise effect of the optical router. As the number of signal paths in the communication increases, the secondary crosstalk effect increases because noise accumulates and propagates along the signal path.

The process of the EWOSA is described in Algorithm 2. In lines 1 and 2, all possible signal paths are first selected as  $P_S$ s. Lines 4–7 then set the search range to search for  $P_X$  through a predefined  $P_X$  searching algorithm. Here, several subsets are created according to the priority of the searching condition, and these subsets reduce the possibility of the algorithm falling into the local minimum. Lines 8–9 select

**Algorithm 2** Worst-CASE OSNR Searching Algorithm

```

1: for i = 0 to max_signal_path do // loop1 for PS
2:   select PS[i] from all possible signal paths
3:   for j = 0 to max_signal_path do // loop2 for PX
4:     for k = 0 to max_candidate do // loop3 for scan range
5:       if the difference between crosstalk powers of
           PX[k] and PX[k-1] < crosstalk
           threshold do
6:         add PX[k] selected by the PX searching
           condition to the scan range
7:         calculate the OSNR of PX[k]
8:       else
9:         replace PX[j] with the signal path that
           causes the minimum OSNR among the signal
           paths in the scan range
10:        break loop3
11:      end if
12:    end for
13:    if current OSNR ≥ OSNR of (j - 1)th PS
        or there are no more PXs to search do
14:      break loop2
15:    end if
16:  end for
17:  if current OSNR < previous OSNR do
18:    update the minimum OSNR
19:  end if
20: end for

```

the signal path that causes the minimum OSNR in the corresponding  $P_X$  scan range. Here, if multiple  $P_X$ s cause the minimum OSNR, the shortest  $P_X$  is selected. This process is repeated until there are no more  $P_X$ s that lower the OSNR through the condition in line 13. Finally, in line 17, the signal paths causing the lowest OSNR among the  $P_S$  and  $P_X$  group pairs are selected, and the OSNR is regarded as the worst-case OSNR and is recorded.

3) SEARCHING FOR WORST-CASE OSNR

Considering the  $P_X$ s selected in step 2 among the selected  $P_S$  candidates, the communication patterns of the  $P_S$  and  $P_X$ s that induce minimum OSNR are selected as the signal paths causing the worst-case OSNR, and the corresponding minimum OSNR becomes the worst-case OSNR. The EWOSA finally records the corresponding signal paths and the worst-case OSNR.

Here, we describe applying the EWOSA to an ONoC using partial routing with a widening bandwidth using WDM. Fig. 7 shows the Crux router architecture of a WDM-based ONoC using  $W$  wavelengths. Because MR switches with different resonance frequencies are required for each allocated wavelength, the number of MRs required for each switching increases by the number of wavelengths. Therefore, the OSNR  $OSNR^{\lambda_n}$  for the wavelength  $\lambda_n$  can be expressed as (6).

$$OSNR^{\lambda_n} = 10 \log(P_S^{\lambda_n} / P_N^{\lambda_n}) \tag{6}$$

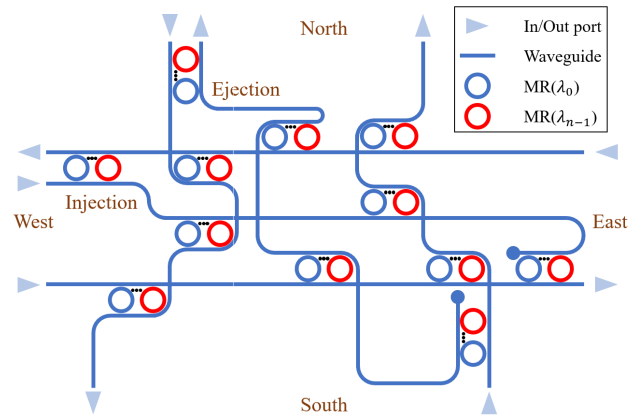


**FIGURE 7.** Crux router architecture in a WDM-based ONoC.

Assuming that  $W$  wavelengths have the same spacing in a given free spectral range (FSR), the spacing between two consecutive wavelengths  $\lambda_n$  and  $\lambda_{n+1}$  is the same ( $FSR/W$ ). Therefore,  $\lambda_n$  is calculated using (7).

$$\lambda_n = \lambda_0 + (n - 1) \cdot (FSR/W) \tag{7}$$

Thus, the following equation (8) holds for the resonance wavelength  $\lambda_{MR_m}$  of the  $m^{th}$  MR:

$$\lambda_{MR_m} = \lambda_{MR_0} + (m - 1) \cdot (FSR/W). \tag{8}$$

$\lambda_0$  and  $\lambda_{MR_0}$  can be determined by the system designer. In this study, we assume that  $\lambda_0 = \lambda_{MR_m}$ . The intensity  $\psi(\lambda_n, \lambda_{MR_m})$  at which the wavelength  $\lambda_n$  interferes with an MR, whose resonance wavelength is  $\lambda_{MR_m}$ , is as shown in (9):

$$\psi(\lambda_n, \lambda_{MR_m}) = \delta^2 / (\lambda_n - \lambda_{MR_m})^2 + \delta^2 \tag{9}$$

where  $\delta = \lambda_{MR_m} / 2Q$ .

Because we assume that  $\lambda_0 = \lambda_{MR_0}$ , the degree of interference between wavelengths is determined by the quality factor  $Q$ , the resonance wavelength  $\lambda_{MR_m}$ , and the number of wavelengths  $W$ . The EWOSA receives the number of given wavelengths,  $FSR$ ,  $Q$ , and  $\lambda_{MR_0}$  as the input parameters. Subsequently, it prepares an LUT for each wavelength and calculates the OSNR accordingly.

For example, assuming that  $\lambda_0$  and  $\lambda_{MR_0}$  are both 1550 nm, the  $FSR$  is 30 nm, and the  $Q$  factor is 9000 in a WDM-based ONoC using eight wavelengths. The intensity  $\psi(\lambda_0, \lambda_{MR_1})$  that interferes with the corresponding MR can be obtained as  $5.30 \times 10^{-4}$ .

In summary, the EWOSA is composed of three steps, and the operation of the algorithm in each step is designed to achieve the desired goal. In step 2, the communication patterns that minimize the OSNR of each candidate are determined through a semi-greedy approach. Multiple subsets that are created through the priorities of various searching conditions reduce the possibility that the algorithm falls into the local minimum. Finally, in step 3, the candidate that causes the minimum OSNR among the candidate groups is determined as the worst case.



TABLE 1. Parameters of optical elements.

| Parameter   | Value         | Parameter   | Value   |
|-------------|---------------|-------------|---------|
| $L_C$       | -0.04 dB      | $L_{p,on}$  | -0.5 dB |
| $L_p$       | -0.274 dB/cm  | $K_C$       | -40 dB  |
| $L_{c,off}$ | -0.04 dB      | $K_{p,off}$ | -20 dB  |
| $L_{c,on}$  | -0.5 dB       | $K_{p,on}$  | -25 dB  |
| $L_b$       | -0.005 dB/90° | $K_r$       | ≈ 0     |
| $L_{p,off}$ | -0.005 dB     | $K_t$       | -50 dB  |

IV. EVALUATION

We configured various network environments to verify the EWOSA and all the algorithms including the proposed algorithm were implemented using the C++ programming language. For a fair comparison, the same parameters and coefficients were applied in all the simulations. The waveguide used in all the networks was 450 nm × 200 nm, the insertion loss was assumed to be 0.274 dB/cm, and the bending and crossing losses were assumed to be -0.005 dB/90° and -0.04 dB, respectively [17], [18]. The other coefficients of the insertion loss and crosstalk noise are presented in Table 1 [10].

We analyzed the OSNR and runtime of the mesh-based and fat-tree-based ONoCs. Here, the length of the waveguide in the router was considered to be the minimum value, considering the diameters of the MR switch and optical terminator. The diameters of the MR switch and optical terminator were assumed to be 10 μm and 15 μm, respectively [15]. The output power of the laser was assumed to be 0 dB, and the lengths of the waveguide between the routers and the waveguide between the laser and router were ignored. Additionally, we simulated the OSNR of networks using WDM and SOA, which increased the bandwidth and power efficiency of the ONoC to verify the generality of the EWOSA.

This analysis primarily aimed to verify how the EWOSA can improve the accuracy of the worst-case OSNR and operate at a low runtime compared with the previous studies by considering the signal path of various crosstalk noises. Therefore, the proposed algorithm was verified through the accuracy and runtime analysis of the worst-case OSNR in each network environment.

A. OSNR ANALYSIS

Table 2 shows the worst-case OSNR analyzed with network sizes ranging from 8 × 8 to 16 × 16 in ONoCs with mesh topology compared with the formal worst-case (FWC) described in [10] in a single wavelength environment. For a network size of 8 × 8, the worst-case OSNR of the FWC was approximately 3.27 dB, and the worst-case OSNR of the EWOSA was approximately 3.09 dB; hence, the worst-case OSNR obtained through the EWOSA was approximately 0.18 dB lower. When the network sizes were 16 × 16, the worst-case OSNRs determined by the EWOSA were lower than the FWC by 0.12 dB. As the network size increased, the difference between the worst-case OSNRs

TABLE 2. OSNR comparison results for mesh-based ONoC.

| Network size | Signal power |       | Noise power |       | worst-case OSNR |       |
|--------------|--------------|-------|-------------|-------|-----------------|-------|
|              | FWC          | EWOSA | FWC         | EWOSA | FWC             | EWOSA |
| 8 × 8        | -3.38        | -3.43 | -6.65       | -6.15 | 3.27            | 3.09  |
| 12 × 12      | -4.62        | -4.45 | -4.78       | -4.49 | 0.16            | 0.04  |
| 16 × 16      | -5.86        | -5.69 | -3.72       | -3.44 | -2.14           | -2.25 |

W: number of wavelengths

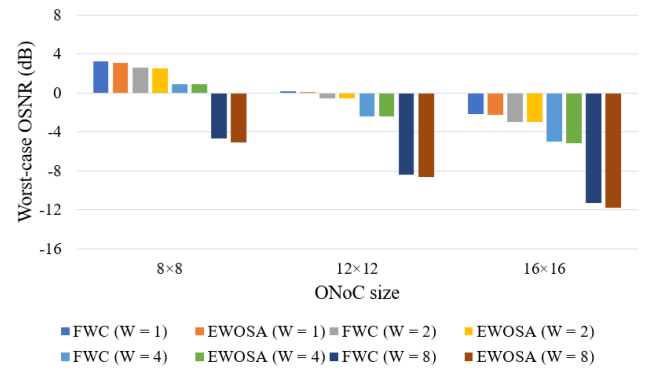


FIGURE 8. OSNR comparison results for mesh-based ONoC with WDM (W: the number of wavelengths).

of the FWC and EWOSA decreased. This tendency was because, from a network with a size of 12 × 12 or more, the increase in noise power decreases while the amount of decrease in signal power is constant in Table 2. As the length of the  $P_S$  increases as the network size increases, insertion loss increases constantly, but the number of nodes where crosstalk noise can be introduced increases slightly; hence, the effect of the added crosstalk noise decreases.

The results of the worst-case OSNR analysis are presented in Fig. 8 when the number of wavelengths for the 8 × 8 to 16 × 16 networks with mesh topology ranged from 1 to 8 in a WDM-based ONoC. The quality factor  $Q$  and the lowest wavelength  $\lambda_0$  were assumed to be 9000 and 1550 nm, respectively. Additionally, we assumed that the insertion loss and crosstalk noise of each optical signal, except for the inter-wavelength interference, followed the values in Table 1. When the number of wavelengths was 1, 2, 4, and 8, the improvements in the worst-case OSNR obtained from the EWOSA compared with the FWC for all the network sizes were 0.09 dB, 0.09 dB, 0.11 dB, and 0.17 dB, respectively. This tendency implies that the accuracy of the EWOSA enhances as the number of wavelengths increases. As the number of wavelengths increases, the input-to-output ratio of signal and noise power of the optical router changes due to the increased MRs and the changed structure of the router. Therefore, the EWOSA, which is designed to flexibly respond to ONoC conditions and environmental changes, calculates more accurate worst-case OSNR than the FWC. Table 2 and Fig. 8 indicate that the larger the network size, the lower the difference between the worst-case OSNRs obtained from the FWC and EWOSA.

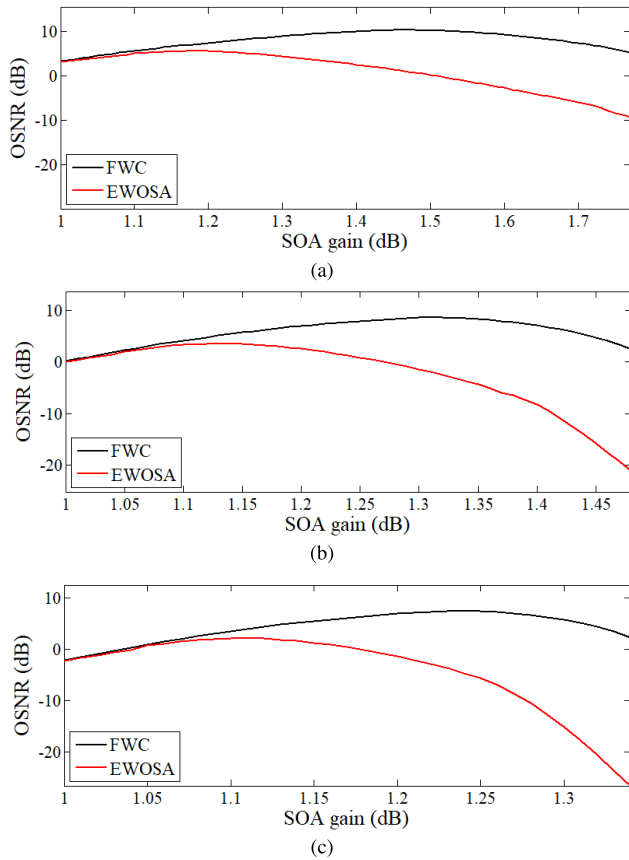


FIGURE 9. OSNR comparison results for mesh-based ONoCs with network sizes (a) 8 × 8, (b) 12 × 12, and (c) 16 × 16.

Fig. 9 shows the results of analyzing the worst-case OSNR in each network according to the network size and gain of SOA when the SOAs were arranged using the SOA deployment algorithm proposed in [16]. When the gain of the SOA became larger than a specific value that indicated the ideal gain, the worst-case OSNR was lowered because of an excessive amplification of crosstalk. In the 8 × 8 network, the ideal gain with the highest worst-case OSNR analyzed by the EWOSA differed by 0.28dB from the FWC, and the worst-case OSNR was 4.81 dB. In the 12 × 12 and 16 × 16 networks, the EWOSA could determine OSNRs that differed by as much as 5.09 dB and 5.39 dB, respectively, from the FWC. The worst-case OSNR indicated a considerable difference from the network to which the SOA deployment technique was not applied. This was because, depending on the SOA arrangement, the worst-case does not occur in the longest path and the scenario considering the amplification of the SOA becomes the worst case. In other words, the EWOSA analyzed the worst-case OSNR and enabled a more accurate SOA gain setting in the SOA deployment stage.

We performed OSNR analysis when the proposed EWOSA was applied to a fat-tree-based ONoC. As with the mesh-based topology, the insertion loss and crosstalk coefficients of the MR were the same as those listed in Table 1. We used an OTAR, which was proposed in [8]. Furthermore, the network structure and routing method used were waveguide-crossing

TABLE 3. OSNR comparison results for fat-tree-based ONoC.

| Network size | The EWOSA | [8]      |
|--------------|-----------|----------|
| 32           | 4.88 dB   | 5.66 dB  |
| 64           | 3.01 dB   | 3.60 dB  |
| 128          | 1.25 dB   | 2.22 dB  |
| 256          | -6.21 dB  | -5.50 dB |

TABLE 4. Runtime results for mesh-based ONoC.

| Network size | Runtime(sec)  |           |           |           |
|--------------|---------------|-----------|-----------|-----------|
|              | EWOSA (W = 1) | EWOSA (2) | EWOSA (4) | EWOSA (8) |
| 8 × 8        | 35.27         | 50.82     | 68.74     | 119.05    |
| 16 × 16      | 1216.52       | 1635.79   | 1647.74   | 2886.22   |
| 24 × 24      | 7840.64       | 12901.64  | 15264.11  | 30406.85  |
| 32 × 32      | 37647.49      | 48517.03  | 61565.03  | 91262.69  |

W: the number of wavelengths

loss-optimized ONoC and insertion-loss-minimized source-index deterministic routing (SIDR), respectively, which were used in [19]. SIDR minimizes the insertion loss while maintaining the load balancing characteristic in fat-tree-based ONoCs. The OSNR and runtime according to network size are shown in Table 3. The average worst-case OSNR of the EWOSA was observed to be 0.76 dB lower than the average value of the fat-tree-based ONoCs analyzed in [8]. Meanwhile, for the fat-tree-based ONoC, we observed that the OSNR decreased rapidly as the network size increased so that the scalability was lower than that of the mesh-based ONoC. This tendency occurred because the number of routers used in the mesh-based ONoC was the same as the number of processor cores, whereas the number of routers used in the fat-tree-based ONoC increased as the number of processor cores increased.

Based on these results, the accuracy of determining the worst-case OSNR of the EWOSA and the generality was concluded to be high. In the following subsection, the runtimes of the EWOSA are analyzed.

### B. RUNTIME ANALYSIS

The runtime of the EWOSA is shown in Table 4 according to the number of wavelengths in the mesh-based ONoC. The EWOSA required tens of seconds to tens of hours depending on the network size, but this is acceptable at the front end of the design. As the number of wavelengths used by the WDM increased, the number of MRs increased, and consequently, the number of iterations increased owing to resonance. Accordingly, the total amount of computations increased in proportion to the number of wavelengths. Thus, the runtime increased.

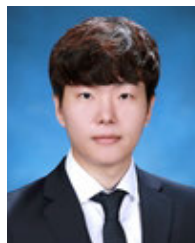
### V. CONCLUSION

The worst-case OSNR is a critical metric in evaluating the total power consumption of ONoCs. We established an

extended worst-case OSNR searching algorithm to be applicable for a wide range of topologies and network sizes. By in-depth inspection of the crosstalk noise and insertion loss, including secondary effects, the EWOSA provides a more rigorous worst-case OSNR analysis capability than previous studies with reasonable computational complexity. Furthermore, the EWOSA can be used in the OSNR optimization step of ONoCs and accommodate ONoCs with WDM functionality and SOAs.

## REFERENCES

- [1] S. Werner, J. Navaridas, and M. Luján, "A survey on optical network-on-chip architectures," *ACM Comput. Surv.*, vol. 50, no. 6, pp. 1–37, Jan. 2018.
- [2] H. Jia, T. Zhou, Y. Zhao, Y. Xia, J. Dai, L. Zhang, J. Ding, X. Fu, and L. Yang, "Six-port optical switch for cluster-mesh photonic network-on-chip," *Nanophotonics*, vol. 7, no. 5, pp. 827–835, May 2018.
- [3] Y. Xie, W. Xu, W. Zhao, Y. Huang, T. Song, and M. Guo, "Performance optimization and evaluation for torus-based optical Networks-on-Chip," *J. Lightw. Technol.*, vol. 33, no. 18, pp. 3858–3865, Sep. 15, 2015.
- [4] E. Fusella and A. Cilaro, "Crosstalk-aware automated mapping for optical networks-on-chip," *ACM Trans. Embedded Comput. Syst.*, vol. 16, no. 1, pp. 1–26, Nov. 2016.
- [5] I. G. Thakkar, S. V. R. Chittamuru, and S. Pasricha, "Run-time laser power management in photonic NoCs with on-chip semiconductor optical amplifiers," in *Proc. 10th IEEE/ACM Int. Symp. Netw.-Chip (NOCS)*, Sep. 2016, pp. 1–4.
- [6] P. K. Hamedani, N. E. Jerger, and S. Hessabi, "QuT: A low-power optical network-on-chip," in *Proc. 8th IEEE/ACM Int. Symp. Netw.-Chip (NoCS)*, Sep. 2014, pp. 80–87.
- [7] H. Gu, K. H. Mo, J. Xu, and W. Zhang, "A low-power low-cost optical router for optical networks-on-chip in multiprocessor systems-on-chip," in *Proc. IEEE Comput. Soc. Annu. Symp. VLSI*, May 2009, pp. 19–24.
- [8] H. Gu, J. Xu, and W. Zhang, "A low-power fat tree-based optical network-on-chip for multiprocessor system-on-chip," in *Proc. Design, Autom. Test Eur. Conf. Exhib.*, Apr. 2009, pp. 3–8.
- [9] M. Nikdast, J. Xu, L. H. K. Duong, X. Wu, X. Wang, Z. Wang, Z. Wang, P. Yang, Y. Ye, and Q. Hao, "Crosstalk noise in WDM-based optical networks-on-chip: A formal study and comparison," *IEEE Trans. Very Large Scale Integr. (VLSI) Syst.*, vol. 23, no. 11, pp. 2552–2565, Nov. 2015.
- [10] Y. Xie, M. Nikdast, J. Xu, X. Wu, W. Zhang, Y. Ye, X. Wang, Z. Wang, and W. Liu, "Formal worst-case analysis of crosstalk noise in mesh-based optical networks-on-chip," *IEEE Trans. Very Large Scale Integr. (VLSI) Syst.*, vol. 21, no. 10, pp. 1823–1836, Oct. 2013.
- [11] Y. Xie, J. Xu, J. Zhang, Z. Wu, and G. Xia, "Crosstalk noise analysis and optimization in  $5 \times 5$  hitless silicon-based optical router for optical networks-on-chip (ONoC)," *J. Lightw. Technol.*, vol. 30, no. 1, pp. 198–203, Jan. 2012.
- [12] M. Nikdast, J. Xu, X. Wu, W. Zhang, Y. Ye, X. Wang, Z. Wang, and Z. Wang, "Systematic analysis of crosstalk noise in folded-torus-based optical networks-on-chip," *IEEE Trans. Comput.-Aided Design Integr. Circuits Syst.*, vol. 33, no. 3, pp. 437–450, Mar. 2014.
- [13] Y. Xie, M. Nikdast, J. Xu, W. Zhang, Q. Li, X. Wu, Y. Ye, X. Wang, and W. Liu, "Crosstalk noise and bit error rate analysis for optical network-on-chip," in *Proc. 47th Design Autom. Conf.*, Jun. 2010, pp. 657–660.
- [14] M. S. Kim, Y. W. Kim, and T. H. Han, "System-level signal analysis methodology for optical network-on-chip using linear model-based characterization," *IEEE Trans. Comput.-Aided Design Integr. Circuits Syst.*, early access, Oct. 4, 2019, doi: [10.1109/TCAD.2019.2945709](https://doi.org/10.1109/TCAD.2019.2945709).
- [15] L. Zhou and A. W. Poon, "Silicon electro-optic modulators using pin diodes embedded 10-micron-diameter microdisk resonators," *Opt. Express*, vol. 14, no. 15, pp. 6851–6857, Jul. 2016.
- [16] J. Y. Jang, "Power and signal-to-noise ratio optimization in mesh-based hybrid optical network-on-chip using semiconductor optical amplifiers," *Appl. Sci.*, vol. 9, no. 6, pp. 1–23, Mar. 2019.
- [17] F. Xia, L. Sekaric, and Y. Vlasov, "Ultracompact optical buffers on a silicon chip," *Nature Photon.*, vol. 1, no. 1, pp. 65–71, Dec. 2006.
- [18] W. Ding, D. Tang, Y. Liu, L. Chen, and X. Sun, "Compact and low crosstalk waveguide crossing using impedance matched metamaterial," *Appl. Phys. Lett.*, vol. 96, no. 11, pp. 111114.1–111114.3, Mar. 2010.
- [19] J. H. Lee, M. S. Kim, and T. H. Han, "Insertion loss-aware routing analysis and optimization for a fat-tree-based optical network-on-chip," *IEEE Trans. Comput.-Aided Design Integr. Circuits Syst.*, vol. 37, no. 3, pp. 559–572, Mar. 2018.
- [20] M. Luo, "Current sensor based on an integrated micro-ring resonator and superparamagnetic nanoparticles," *Opt. Express*, vol. 28, no. 4, pp. 5684–5691, Feb. 2020.



**YONG WOOK KIM** (Student Member, IEEE) received the B.S. degree in electronic and electrical engineering from Sungkyunkwan University, Suwon, South Korea, in 2016, where he is currently pursuing the M.S. and Ph.D. degrees in electrical and computer engineering. His research interests include NoC, machine learning, and computer architecture.



**JAE HOON LEE** (Member, IEEE) received the B.S. degree in semiconductor systems engineering and the M.S. and Ph.D. degrees in electronic, electrical, and computer engineering from Sungkyunkwan University, Suwon, South Korea, in 2011, 2014, and 2018, respectively. Since 2018, he has been with the Memory Division, Samsung Electronics, South Korea, where he has worked on HBM and in-memory processing unit design. His research interests include SoC design methodology and high-performance bus architecture.



**TAE HEE HAN** (Member, IEEE) received the B.S., M.S., and Ph.D. degrees in electrical engineering from the Korea Advanced Institute of Science and Technology (KAIST), Daejeon, South Korea, in 1992, 1994, and 1999, respectively. From 1999 to 2006, he was with the Telecom Research and Development Center, Samsung Electronics, where he developed 3G wireless, mobile TV, and mobile WiMax handset chipsets. Since March 2008, he has been with Sungkyunkwan University, Suwon, South Korea, as a Professor. From 2011 to 2013, he had served as a full-time Advisor on system ICs for the Korean Government. His current research interests include SoC architecture for artificial intelligence, emerging memory systems, embedded software, deep learning, NVM, PIM, and NoC.

...